ISIJ International, Vol. 46 (2006), No. 9, pp. 1354–1360

Continuous Cooling Transformation Temperature and Microstructures of Microalloyed Hypereutectoid Steels

A. M. ELWAZRI,[1)] P. WANJARA[2)] and S. YUE[1)]

1) McGill University, Department of Mining, Metals and Materials Engineering, 3610 University Street, Montréal, Québec, Canada, H3A 2B2. 2) National Research Council of Canada, Institute for Aerospace Research, Aerospace Manufacturing Technology Center, 5145 Decelles Avenue, Montréal, Québec, H3T 2B2. E-mail: abdelbaset.el-wazri@mcgill.ca

(*Received on January 12, 2006; accepted on June 21, 2006*)

The transformation behavior under continuous cooling conditions was investigated for four hypereutectoid steels of 1 % carbon with different microalloying additions of vanadium and silicon. Continuous cooling compression testing of the hypereutectoid steels was employed to study the influence of processing conditions (re-heat temperature), microstructure (prior-austenite grain size) and chemical composition (vanadium and silicon) on the critical transformation temperature (A_{r3}). Overall, for the hypereutectoid steel compositions examined, the transformation temperatures were determined to be relatively stable, with a variation of roughly 15°C when the reheat temperature was changed from 1 000 to 1 200°C. The addition of microalloying elements such as vanadium and silicon was determined to increase the austenite-to-pearlite transformation start temperature of the hypereutectoid steels by about 10–30°C. These changes in the transformation behavior observed with decreasing re-heating temperature and microalloying additions were related to microstructural changes in the hypereutectoid steels, such as prior-austenite grain size refinement, carbide precipitation and grain boundary cementite fragmentation.

KEY WORDS: continuous cooling compression testing; transformation temperature; microalloyed hypereutectoid steels; vanadium; silicon.

1. Introduction

To design heat treatment and thermomechanical schedules for processing hypereutectoid ferrous materials, the various critical transformation temperatures must be considered. One of these is the no recrystallization temperature (T_{nr}) that defines the "holding phase" for the controlled rolling of microalloyed steels that is applied for tailoring the microstructural characteristics to obtain optimized mechanical properties.[1)]. As important are the austenite-to-pearlite transformation (and *vice versa*) start and finish temperatures that under equilibrium conditions are referred to as the A_{e3} and A_{e1}, respectively. Since under industrial processing conditions the austenitic phase is subjected to continuous cooling (or heating), the transformation to pearlite usually differs from equilibrium and is retarded to lower start and finish temperatures, referred to as the A_{r3} and A_{r1}, respectively. Alternatively, on continuous heating from the pearlite region, the transformation to austenite is postponed to higher start and finish temperatures, referred to as A_{c3} and A_{c1}. It is noteworthy that in the interval between the equilibrium and non-equilibrium critical temperatures, the austenite or pearlite phase in the hypereutectoid steel is in the metastable state.[2,3)]

To determine the non-equilibrium critical transformation temperatures during cooling, previous work has indicated that the A_{r3} can be obtained using different laboratory techniques, including thermal analysis, dilatometry, torsion testing and continuous cooling compression (CCC) testing.[1,4–9)] For the interest of thermomechanical processing, although both the torsional and CCC physical simulation techniques have the advantage of characterizing the transformation behavior of the material in the microstructural condition immediately after the application of the hot working schedule, the latter has been recognized for having a greater sensitivity for A_{r3} measurement.[4,6)] Over the years, the various physical simulation studies on hypoeutectoid and eutectoid steel compositions have been instrumental in determining the specific value for the non-equilibrium critical temperatures for the transformation of austenite-to-ferrite for different material and processing conditions, such as the cooling rate, chemical composition, and microstructure.[1,6,7,10,11)] For hypereutectoid steels, where the decomposition of austenite begins with a rapid nucleation and high growth rate of pearlite, the critical transformation temperatures for the diffusional formation of alternating lamellae of ferrite and cementite at austenite grain boundaries[12–16)] must be examined systematically for the influence of materials and processing conditions. In particular, the determination of the austenite-to-pearlite transformation start temperature is important for achieving microstructural control during the thermomechanical processing of hypereutectoid steel grades. In this paper, the research work reported formed part of a larger program on developing the technology for

processing hypereutectoid steel grades through optimized hot working conditions to control the microstructure and mechanical properties. Part of this program involved characterization of the flow behavior under hot rolling conditions and determining the relationship between the microstructure and mechanical properties for various hypereutectoid steel grades.[12,17–21] In the present work, the objective was to determine the effect of deformation in the single-phase austenite and multiple-phase region of austenite, ferrite and cementite on the transformation behavior to pearlite for various hypereutectoid steel compositions.

2. Experimental Procedure

2.1. Materials

Three hypereutectoid steels (A, B and C) with varying silicon, vanadium and nitrogen contents were prepared at CANMET Materials Technology Laboratory (Ottawa, Ontario, Canada), using vacuum melting. A fourth hypereutectoid steel without vanadium (D), used as a reference, was provided by IVACO Rolling Mills (L'Orignal, Ontario, Canada). The chemical compositions of these steels are given in **Table 1**. From each steel, cylindrical specimens were machined to have dimensions of 11.4 mm in height and a 1.5 height-to-diameter ratio.

2.2. Continuous Cooling Compression (CCC) Testing

The dynamic transformation of austenite-to-pearlite in the hypereutectoid steel grades was followed using CCC testing,[4] which is based on the principal concept that different phases react to deformation in differing ways. For instance, using the general form of the constitutive equation and the expression for the calculation of the high temperature flow strength,[22,23] the hypothetical flow stress behavior for material deformation in the single-phase austenite region increases smoothly with decreasing temperature,[4,7] as indicated by curve A in **Fig. 1**. Under practical conditions, any deviation (or deflection) from this behavior can be related to a microstructural change. Curve B represents the flow stress behavior of the hypereutectoid material deforming in the pearlite phase field. The transition region between curves A and B then represents the flow stress behavior of the hypereutectoid material deforming in the austenite+pearlite multiple phase fields. Hence, by the applying the CCC technique, the temperature corresponding to the first cooling transition point (or A_{r3}) can be determined to obtain the start of the austenite-to-pearlite transformation in the hypereutectoid steel materials.

The CCC testing of the hypereutectoid steels was performed on a computerized Materials Testing System (Model 810) adapted for high temperatures. The equipment consists of a load frame rated for a maximum load of 25 kN and a closed loop hydraulic power supply with a computerized control system. The high temperatures were attained with a Research Incorporated radiant furnace, interfaced with a computer control system that is used to generate commands, record data and perform real-time decision making during testing. After the completion of each test, the load and displacement data were transferred to a personal computer for analysis. During CCC testing, thin sheets of mica (50–80 μm thick), separated by a layer of boron nitride powder, were placed between the face of the specimens and the anvils in order to maintain uniform deformation and avoid sticking problems during quenching. The specimen and the anvils were enclosed within a quartz tube, in which argon gas was passed to prevent oxidation of the specimen.

Table 1. Chemical composition of experimental steels (mass%).

	C	*Si*	*Mn*	*Cr*	*Ni*	*Cu*	*V*	*P*	*S*	*N*
A	1.1	0.23	0.63	0.04	0.038	0.036	0.17	0.010	0.007	0.007
B	1.0	0.99	0.77	0.066	0.039	0.037	0.078	0.008	0.008	0.013
C	1.08	0.78	0.75	0.049	0.039	0.037	0.26	0.009	0.009	
D	0.91	0.22	0.49	0.04	0.07	0.02		0.006	0.005	0.0031

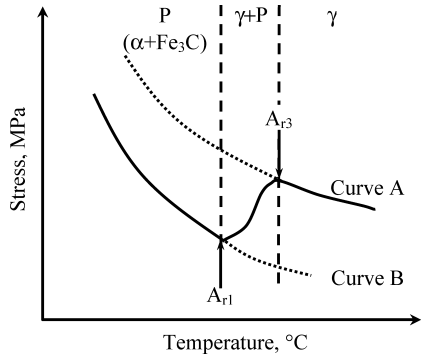

Fig. 1. Schematic illustration of temperature dependence of the CCC flow stress behavior during cooling from the austenite (γ) to the pearlite (P) region.

To characterize the austenite-to-pearlite transformation, CCC testing was performed by heating the steel specimens to the austenitizing (or re-heating) temperature between 1 000 and 1 200°C, holding for 20 min for thermal stabilization and followed by cooling at a constant rate of $1°C \cdot s^{-1}$ to 850°C. At this temperature, continuous deformation at a constant strain rate of $0.001\,s^{-1}$ was applied to the specimen while maintaining cooling at a rate of $1°C \cdot s^{-1}$. The true stress and true strain values were calculated from the load-displacement data generated during deformation. The A_{r3} temperature was calculated from the strain value at the first cooling transition point in the flow stress-strain data for the various hypereutectoid steel grades (using the values for constant cooling and strain rate).

2.3. Microstructures

In order to determine the initial austenite grain sizes of the materials tested, a series of specimens were heat treated to the austenitizing (or re-heating) temperature between 1 000 and 1 200°C, followed by quenching in water. The quenched specimens were mounted in bakelite, and automatically prepared by grinding using successively finer silicon carbide paper from 60 to 800 grit and fine polishing with 9, 3 and 1 μm diamond solutions. The prior austenite grain boundaries were delineated by immersing in a saturated picric acid solution (containing 4 drops HCl and 10 drops wetting agent Teepol per 100 mL saturated aqueous picric acid) and swabbed regularly with cotton wool to remove the dark deposit formed due to the chemical attack. The grain sizes were determined by the intercept method (ASTM E112).

In addition, to microscopically verify that the start and finish of the austenite-to-pearlite transformation corre-

sponds to the transition points in the flow stress-strain plots obtained for the various hypereutectoid steels, the CCC tests were interrupted after each deviation and quenched within 1 second. Preparation for optical metallography was similar to that described above for grain size analysis, except that the general microstructures of the hypereutectoid steels were revealed by immersing the specimens in a 2% nital etching solution.

3. Results and Discussion

3.1. Stress–Strain Curve of CCC Test

The true stress–true strain behaviors in CCC for the hypereutectoid steels re-heated to 1 200°C are given in **Fig. 2**. As expected from the theoretical analysis of the CCC test (Fig. 1), for each hypereutectoid steel there is an overall increase in the flow stress with increasing strain, *i.e.* decreasing temperature. However, each curve exhibits two deviations from the hypothetical flow stress–temperature behavior: 1) the first cooling transition occurs at a lower strain (or higher temperature) value, followed by 2) a second deflection at a higher strain (or lower temperature) value as indicated in Fig. 2. In particular, it is apparent from the flow stress–strain curves in Fig. 2 that these two specific deviations occur at different temperatures and flow stress levels, which reflect the compositional differences in these microalloyed steels. For instance, the addition of vanadium and silicon (steels A, B, C versus D) was determined to significantly increase the flow stress levels in these steels, especially at temperatures below 800°C. This flow stress increase may be related to the solute drag and solid solution strengthening effects of vanadium and silicon that have been noted to retard dynamic recovery.[24,25]

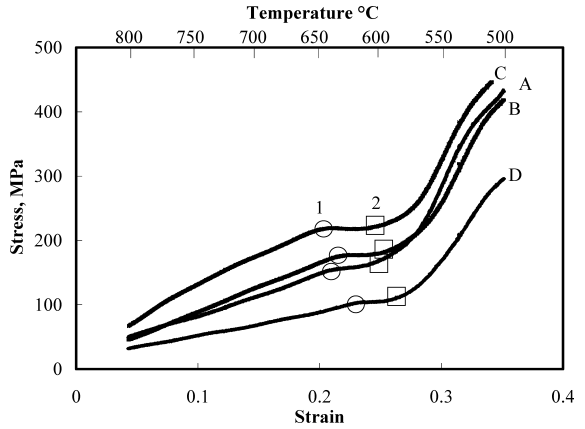

Fig. 2. The CCC true stress–true strain curves for the four hypereutectoid steels re-heated to 1 200°C. The circle and square markers denote the regions where first and second cooling transition points were observed, respectively.

To define the accurate position of each deviation, a linear regression was performed on the data in each region of the curve with deflection points as described by Zarei-Hanzaki *et al.*[4] to exaggerate the transition point. It was determined that the first deviation in Fig. 2. is characterized by a stress drop and a negative slope in the flow stress-strain curve, which indicates that the material is softening. Hence, this first deviation may be related to the start temperature for the transformation of austenite-to-pearlite (A_{r3}), as the latter is softer than the parent phase at any given temperature.[24,26] The second deviation, shown in Fig. 2, was characterized by a change back to a positive slope in the stress–strain curve, and is most probably related to the completion of the austenite transformation (A_{r1}), which then produces a rapid increase in the strengthening rate beyond this transition point.

3.2. Microstructural Verification of the CCC Analysis

As indicated in Fig. 2, there is a change in the slope of the flow stress–strain curves at the first cooling transition point, which was observed to occur at 605, 615, 625 and

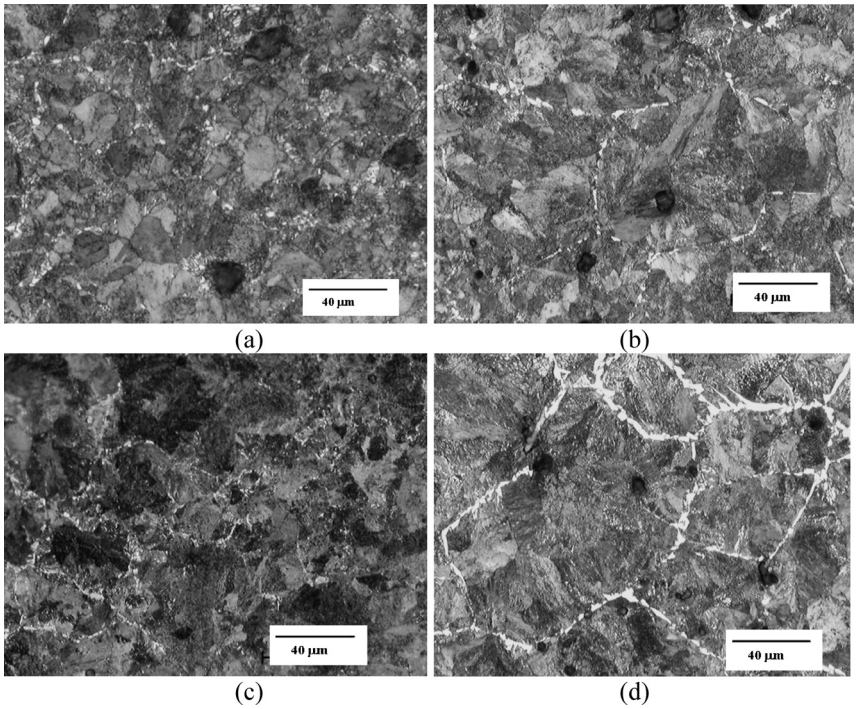

Fig. 3. Optical micrographs showing the microstructure at the austenite-to-pearlite transformation start temperature (A_{r3}): (a) steel A, (b) steel B, (c) steel C and (d) steel D.

632°C for the hypereutectoid steels D, A, B, and C respectively (re-heated at 1 200°C). The microstructures from the CCC tests interrupted and quenched at these first deviation points for the hypereutectoid steels A, B, C, and D are illustrated in **Figs. 3**(a)–3(d), respectively. The resulting microstructures reveal a small volume fraction of pro-eutectoid ferrite or cementite in the form of thin films at the prior-austenite grain boundaries. As this first deviation can be attributed microstructurally to cementite formation, the critical temperatures determined correspond to the austenite-to-pearlite or ferrite transformation start temperature (A_{r3}). It is noteworthy that the thickness of cementite film formed at the prior-austenite grain boundaries is thinner for the microalloyed hypereutectoid steel compositions A, B and C as compared to the reference steel D. Previous work has indicated that the characteristics of the grain boundary cementite film are dependent on the re-heating temperature as well as the vanadium content of the hypereutectoid steel.[12)]

The second change in slope in the flow stress–strain curves, which is indicated as the second transition in Fig. 2, was observed to occur at temperatures of 585, 590, 598 and 602°C for the hypereutectoid steels D, A, B, and C respectively (re-heated at 1 200°C). For the CCC tests interrupted and quenched at the second deviation point, the corresponding microstructures for the hypereutectoid steels A, B, C and D are illustrated in **Fig. 4**(a)–4(d), respectively. As the resulting microstructures for the four hypereutectoid steels are entirely pearlitic, this second deviation can be attributed to the austenite-to-pearlite transformation finish temperature (A_{r1}). From the microstructures it is also apparent that the microalloyed hypereutectoid compositions (steels A, B, and C) have a finer pearlitic structure as compared to the reference steel D. In particular, the various characteristics of the pearlitic structure (nodule size, colony size and interlamellar spacing) have been determined previously to be dependent on both the composition (vanadium and silicon) of the hypereutectoid steel and the re-heating temperature.[11,16)]

3.3. Effect of Re-heat Temperature on A_{r3}

The effect of the reheat temperature on the transformation behavior of the hypereutectoid steels was investigated by plotting the stress–strain–temperature curves using the CCC results for the different austenitizing temperatures, as illustrated in **Fig. 5** for the reference steel D reheated at 1 000°C and 1 200°C. It can be seen that the flow stress in the austenite region increases with increasing reheat temperature, and the difference between the flow stress for reference steel D reheated at 1 000 and 1 200°C was determined to be about 15 MPa. This decrease in flow stress observed with increasing reheat temperature can be attributed to the difference in the prior-austenite grain size between

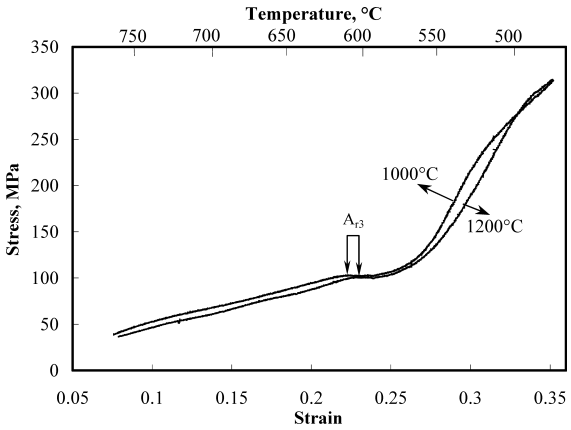

Fig. 5. True stress–strain–temperature curves for steel D after two different reheat temperatures.

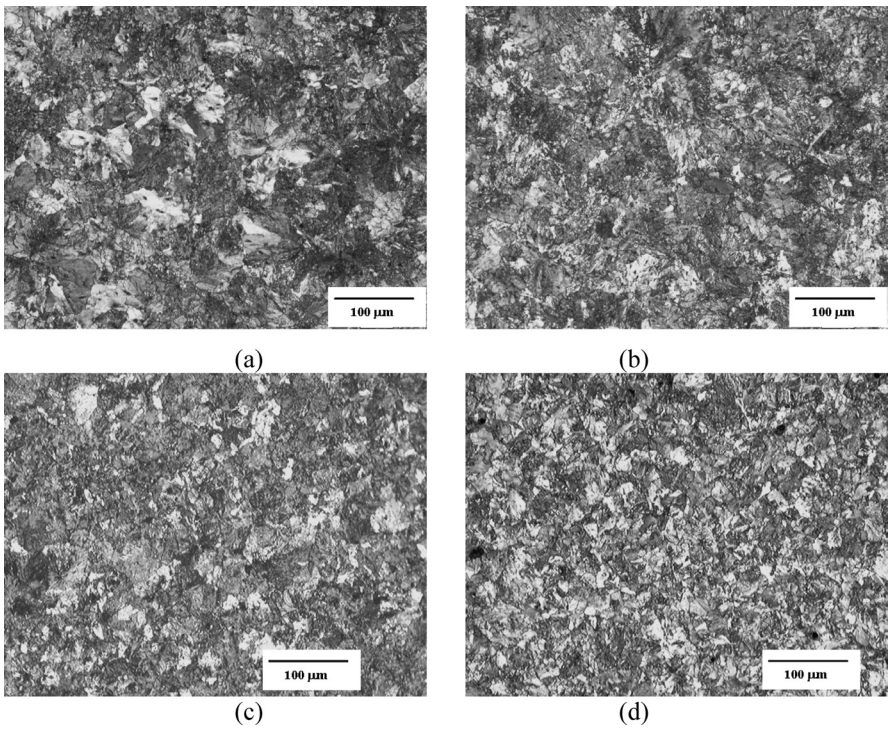

Fig. 4. Optical micrographs showing the microstructure at the austenite-to-pearlite transformation finish temperature (A_{r1}): (a) steel A, (b) steel B, (c) steel C and (d) steel D.

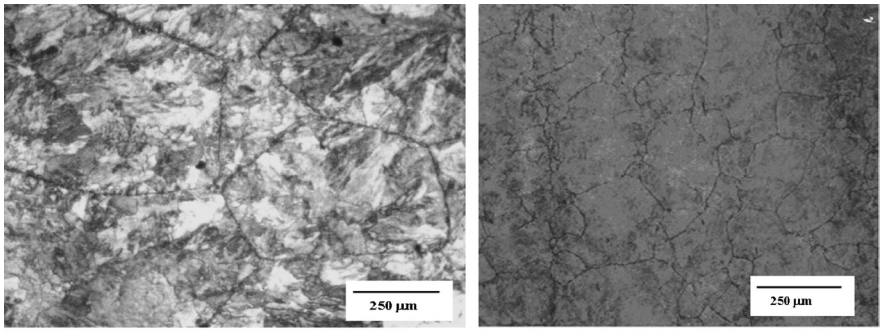

Fig. 6. Reheated austenitic microstructures of steel D.

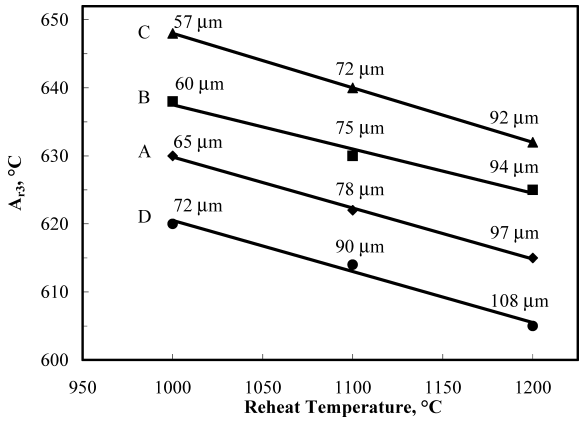

Fig. 7. Effect of reheating temperature on the A_{r3} for the hypereutectoid steels A, B, C and D.

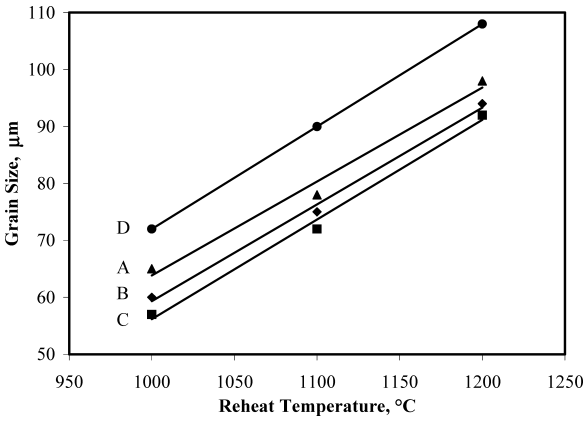

Fig. 8. Effect of austenitizing temperature on the prior-austenite grain size for the hypereutectoid steels A, B, C and D.

1 000 and 1 200°C, as indicated in **Fig. 6**. Measurement of the A_{r3} values for steel D reheated at 1 000 and 1 200°C indicated a difference of roughly 15°C, which may also be related to the change in the prior-austenite grain size between these two temperatures, as indicated in Fig. 6. Specifically, the faster transformation kinetics (or higher A_{r3}) observed for steel D austenitized at 1 000°C is owing to an increased nucleation rate resulting from the finer austenitic grain size relative to reheating conditions at 1 200°C, where increased grain growth during austenitizing and a smaller grain boundary area per unit volume with a concomitant lower nucleation site density necessitate a greater undercooling (or lower A_{r3}) for transformation to pearlite. This finding is consistent with previous work on hypoeutectoid and eutectoid compositions that have determined enhanced kinetics for transformation of refined prior-austenite microstructures to ferrite during isothermal[27] and continuous cooling conditions.[4,6,11,27]

A similar analysis of the CCC results for the microalloyed hypereutectoid compositions was performed to examine the influence of the reheating conditions on the transformation behavior (A_{r3}). As indicated in **Fig. 7**, the transformation of austenite-to-pearlite in the microalloyed hypereutectoid steels appears also to be sensitive to the reheat temperature, as the A_{r3} was observed to increase between 1 200°C and 1 000°C. In particular, a decrease in the reheat temperature from 1 200°C to 1 000°C was observed to increase the A_{r3} by roughly 15°C for each hypereutectoid composition (A, B, C and D) examined. This influence of the reheating conditions on the transformation behavior may also be related to the finer prior-austenite grain size at 1 000°C as compared to 1 200°C. Specifically, decreasing the reheating temperature from 1 200 to 1 000°C was observed to decrease the prior-austenite grain size in the hypereutectoid steels by roughly 32–36 μm, as indicated in **Fig. 8**. Hence, for transformation of austenite to pearlite, the higher critical start temperatures (or lower undercooling) observed for the hypereutectoid steels reheated at 1 000°C is an effect of the enhanced nucleation rate that results due to the larger grain boundary area of the finer prior-austenitic microstructure.

3.4. Effect of Chemical Composition on A_{r3}

The effect of chemical composition on the transformation behavior can be examined from the stress–strain–temperature curves given in Fig. 2 and the plot of the A_{r3} values as a function of the reheating temperature, as given in Fig. 7. As compared to the flow stress behavior of the reference steel D, the microalloyed compositions (steels A, B and C) containing vanadium and silicon additions exhibit considerably higher flow stress levels, as illustrated in Fig. 2 for reheating conditions of 1 200°C. This flow stress increase may be related to two effects: 1) refined prior-austenite grain size and 2) solute drag and solid solution strengthening effects of vanadium and silicon. By comparing the prior-austenite grain size of the microalloyed hypereutectoid compositions with the reference steel D, it is apparent that the austenitic microstructure for each reheat temperature is finer for the former as compared to the latter (Fig. 8). In particular, the results indicate that the prior-austenite

grain size decreases with increasing vanadium content, which can be related to presence of vanadium carbide particles that have an inhibitory effect on grain growth during reheating. This observation agrees with the findings of Han *et al.*[29] that have indicated the inhibition of the austenite growth due to pinning by incompletely dissolved vanadium carbides at the beginning of austenitization or due to the solute drag effects of vanadium, silicon and manganese in hypereutectoid steel compositions. However, it is noteworthy that the difference in the austenitic microstructure within the microalloyed hypereutectoid compositions examined in the present work is not as marked with incremental vanadium additions. Nonetheless, the highest content of vanadium in steel C (0.26%) relative to A (0.17%) and B (0.076%) appears to provide an addition resistance to deformation, most likely due to solute drag and solid solution strengthening effects of the microalloying elements[30] in the hypereutectoid compositions that simultaneously complement the impact of the prior-austenite grain size.

By comparison of the A_{r3} values from the CCC results determined at a constant reheating condition for each hypereutectoid composition, the influence of chemical composition on the austenite-to-pearlite transformation behavior indicated an increase in the transformation kinetics with increasing addition of microalloying elements, as illustrated in Fig. 7. For instance, the A_{r3} values for the hypereutectoid steels D, A, B, and C were determined to be 605, 615, 625 and 632°C, respectively for austenitization at 1 200°C. The observed increase in the austenite-to-pearlite transformation kinetics (or higher A_{r3}) may be related to two effects: 1) refined prior-austenite grain size and 2) precipitation behavior with vanadium and silicon additions. Specifically, it has been remarked that the microalloyed hypereutectoid compositions exhibit a finer prior-austenite grain size, between 32 and 36 μm less than that of reference steel D. This refinement in the prior-austenitic microstructure would then render faster transformation of austenite to pearlite stemming from the enhanced nucleation rate that is associated with the larger grain boundary area in the microalloyed hypereutectoid steels. Nonetheless, since the difference in the austenitic microstructure within the microalloyed hypereutectoid compositions examined in the present work is not as marked with incremental vanadium additions (Fig. 8), the increase in the A_{r3} value observed with increasing vanadium and silicon may be related to the characteristics of the carbide precipitation occurring during cooling. In particular, vanadium microalloying in hypereutectoid steels increases the driving force for carbide nucleation such that there is the presence of vanadium carbides, in small quantities, at the prior-austenite grain boundaries, with the majority of the particulates being precipitated in the grain boundary ferrite.[31] The presence of silicon has also been found to promote the precipitation of vanadium carbides as well as to slow their growth rate and enable the particles to be more finely dispersed.[29] This occurrence of vanadium carbide precipitation has then been observed to have a twofold effect on grain boundary cementite formation.[12,32] An effect of the vanadium carbide formation on the austenite grain boundary is the local depletion of carbon that reduces its diffusion along the boundary to the cementite particles, thereby inhibiting their rapid growth into the boundary and preventing a continuous cementite network.[12] An offset of the carbon being coupled into precipitation is a concomitant promotion of ferrite nucleation and growth, which aids further in inhibiting the continuance of grain boundary cementite.[32] In terms of the transformation kinetics, the presence of the vanadium carbide precipitates appears to encourage the earlier formation of pearlite by acting as nucleation sites as well as enable the fragmentation of grain boundary cementite into particles that in turn augment the nucleation site density. Hence, both silicon and vanadium additions, either separately or in combination, have a noticeable impact on the pearlite nucleation rate such that the transformation kinetics are enhanced by microalloying as demonstrated by the A_{r3} values being 10–30°C greater for the steels A, B and C as compared to the reference steel D (Fig. 7).

4. Conclusions

The application of constant strain rate deformation during continuous cooling can be used to generate flow stress–strain data for the analysis of the austenite transformation characteristics in hypereutectoid steels with and without microalloying additions of vanadium and silicon. The analysis performed in this work demonstrated that the changes in the flow stress–strain behavior determined by CCC testing could be related to microstructural changes that accompany the stages of transformation. Specifically two deviations were observed in the flow stress–strain curves that were related to the austenite-to-pearlite start and finish temperatures in the hypereutectoid steel compositions using microstructural observations for validation. The results from the CCC data analysis were then employed to investigate the effect of compositional, microstructural and processing conditions with the following conclusions:

(1) The austenite-to-pearlite transformation start and finish temperatures of the microalloyed hypereutectoid steels (A, B and C) are about 10 to 30°C higher than reference steel D.

(2) The Ar_3 was found to increase by about 15°C when the reheat temperature was decreased from 1 200 to 1 000°C due to the refinement in the prior-austenitic microstructure that enabled enhanced nucleation and transformation kinetics.

(3) The Ar_3 of the microalloyed hypereutectoid steels was about 10–30°C higher than the reference steel D, which was attributed to the presence of vanadium and silicon that enabled refinement of the prior-austenite grains, vanadium carbide precipitation and fragmentation of the cementite network at the grain boundaries.

Acknowledgements

The authors would like to thank the Canadian Steel Industry Research Association (CSIRA) and the Natural Sciences and Engineering Research Council of Canada (NSERC) for their financial support. The authors are thankful to Professor J.J. Jonas for his beneficial discussions.

REFERENCES

1) N. J. Lourenço, A. M. Jorge, Jr., J. M. A. Rollo and O. Balancin: *Mat. Res.*, **4** (2001), 149.

2) A. M. Elwazri, P. Wanjara and S. Yue: *ISIJ Int.*, **43** (2003), 1080.
3) A. M. Elwazri, P. Wanjara and S. Yue: *Mater. Sci. Eng. A*, **A339** (2003), 209.
4) A. Zarei-Hanzaki, R. Pandi, P. D. Hodgson and S. Yue: *Metall. Trans. A*, **24A** (1993), 2657.
5) M. Eriksson, M. Oldenburg, M. C. Somani and L. P. Karjalainen: *Modelling Simul. Mater. Sci. Eng. A*, **10** (2002), 277.
6) R. Pandi and S. Yue: *ISIJ Int.*, **34** (1994), 270.
7) D. Q. Bai, S. Yue, T. M. Maccagno and J. J. Jonas: *Metall. Mater. Trans. A*, **29A** (1998), 989.
8) I. Kozasu, C. Ouchi, T. Sanpei and T. Okita: Microalloying 75, Union Carbide, New York, (1977).
9) C. R. Mackenzie and R. W. Young: *J. Iron Steel Inst.*, **209** (1971), 918.
10) Y.-K. Lee, J.-M. Hong, C.-S. Choi and J.-K. Lee: *Mater. Sci. Forum*, **475–479** (2005), 65.
11) A. Zarei-Hanzaki, J. Root, P. D. Hodgson and S. Yue: *Acta Metall. Mater.*, **43** (1995), 569.
12) A. M. Elwazri, P. Wanjara and S. Yue: *Metall. Trans. A*, **36A** (2005), 2297.
13) F. C. Hull and R. F. Mehl: *Trans. ASM*, **29** (1942), 381.
14) N. T. Belaiew: *J. Iron Steel Inst.*, **60** (1922), 201.
15) G. E. Pellisier, M. F. Hawkes, W. A. Johnson and R. F. Mehl: *Trans. ASM*, **29** (1942), 1049.
16) F. C. Hull, R. A. Colten and R. F. Mehl: *Trans. AIME*, **150** (1942), 185.
17) A. M. Elwazri, P. Wanjara and S. Yue: *Mater. Sci. Eng. A*, **A404** (2005), 91.
18) A. M. Elwazri, P. Wanjara and S. Yue: *Mater. Sci. Technol.*, **20** (2004), 1469.
19) A. M. Elwazri, P. Wanjara and S. Yue: *CMQ*, **43** (2004), 507.
20) A. M. Elwazri, E. Essadiqi and S. Yue: *ISIJ Int.*, **44** (2004), 162.
21) A. M. Elwazri, E. Essadiqi and S. Yue: *ISIJ Int.*, **44** (2004), 744.
22) G. E. Dieter: Mechanical Metallurgy, 3rd ed., McGraw-Hill Book. Co., New York, (1986), 306.
23) C. M. Sellars and W. J. McTegart: *Acta Metall.*, **14** (1966), 1136.
24) R. W. K. Honeycombe: Steels Microstructure and Properties, Edward Arnold, London, (1981), 34.
25) S. Serajzadeh and A. K. Taheri: *Mat. Lett.*, **56** (2002), 984.
26) S. Zajac, T. Siwecki, W. B. Hutchinson and R. Lagneborg: *Mater. Sci. Forum*, **284–286**, (1998), 295.
27) J. A. Koskiniemi, L. P. Karjalainen, P. G. H. Pistorius and G. T. van Rooyen: *Mater. Sci. Technol.*, **14** (1998), 1115.
28) A. Zarei-Hanzaki: Ph.D. Thesis, McGill University, Montreal, (1994).
29) K. Han, T. D. Mottishaw, G. D. W. Smith, D. V. Edmonds and A. G. Stacey: *Mater. Sci. Eng. A*, **A190** (1995), 207.
30) K. Han, D. V. Edmonds and G. D. W. Smith: *Metall. Mater. Trans. A*, **32A** (2001), 1313.
31) A. M. Elwazri, R. Gavin, P. Wanjara and S. Yue: *Steel Grips*, **2** (2004), 284.
32) K. Han, G. D. W. Smith and D. V. Edmonds: *Metall. Mater. Trans. A*, **26A** (1995), 1617.